Supplement of Solid Earth, 10, 1937–1950, 2019
https://doi.org/10.5194/se-10-1937-2019-supplement

Solid Earth
Open Access

Supplement of

Lithospheric image of the Central Iberian Zone (Iberian Massif) using global-phase seismic interferometry

Juvenal Andrés et al.

Correspondence to: Juvenal Andrés (jandres@ictja.csic.es)

Introduction

In this supplementary document we present complementary information and images regarding the selection of the data used to generate the GloPSI profile. Also, an image comprising the different steps of the post-stack processing is shown. Finally, an explanation of the criteria used to remove the delta pulse of the image at time 0s, accompanied with the corresponding images, is shown. The other considered approaches to solve this problem are discussed. Finally, the list of used earthquakes is included.

Data selection

A total of 81 MW ≥ 5 earthquakes were selected to be processed. The selection of the minimum magnitude to be considered was taken as a balance between the signal quality of the earthquakes and the number of available sources for each deployment.

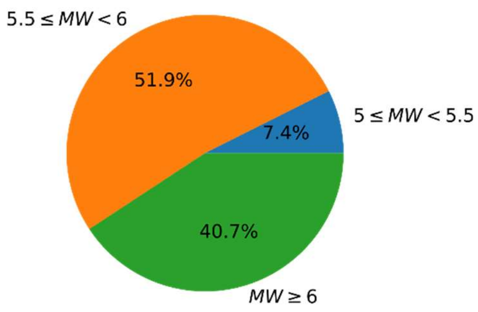

Figure S1. Percentages of events per magnitude for all used earthquakes.

To highlight the importance of including lower magnitude events in the processing, we have created an image of the central deployment only with earthquakes with MW ≥ 6, and compare it to that using all of the available events (Figure S2). In the image with only MW ≥ 6 events, the amplitude and frequency of the autocorrelations it is clearly different, and there is small reflectivity retrieved. This could be due to a lack of information in the stacking process, or due to not retrieving the stationary phase during the stack. This would mean, that these 3 events could interfere destructively in the summation process or that the events do not cover a wide range of ray parameters, needed to produce a quality image.

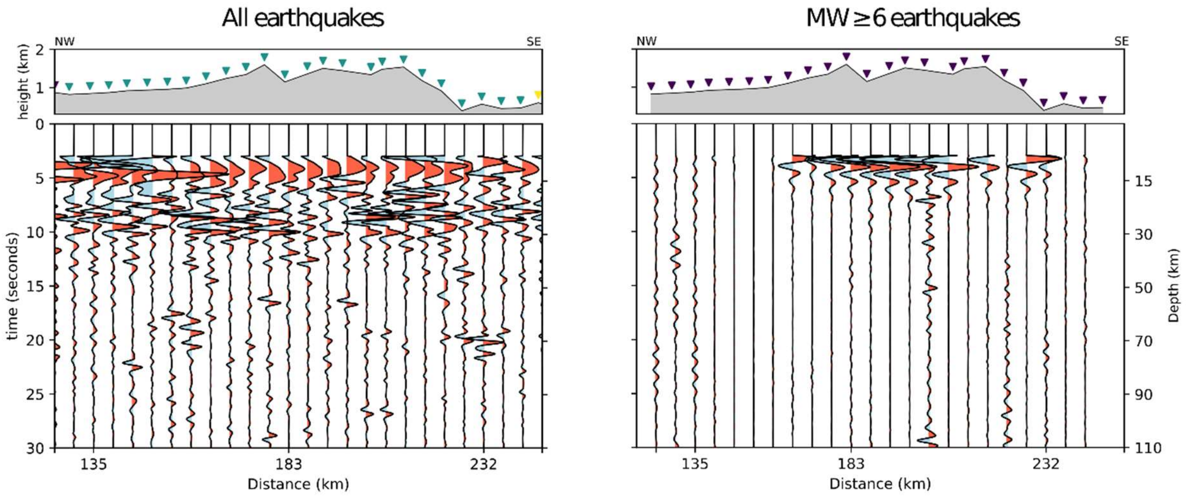

Figure S2. Comparison of the image of the central segment created with all the earthquakes (left) and only with those MW ≥ 6 events (right).

Data processing

The post stack processing applied to generate the zero-offset reflection profile is shown in figure S2.

Step 1 represents the raw stack of the autocorrelations of events for the three deployments, where the delta pulse around t=0 s dominates the image, as its amplitude is much higher than the amplitudes of the rest of the profile.

Step 2 comprises band-pass filtering of the raw stack to enhance higher frequencies and reject the frequencies dominated by the microseism. Therefore, a band-pass filter of 0.7-2 Hz is applied.

In step 3, the dominating delta pulse is muted. The selection of the muting window is based on the entire wavelet (including the positive and negative times of the autocorrelation). The length of the wavelet is 6 s, 3 s positive and 3 s negative times. Therefore, the muting window applied is 3 s.

Delta pulse suppresion

Three different approaches were used in order to eliminate the influence of the delta pulse at time t=0 (Fig. S3).

First deconvolution of the wavelet for each station was tested. For each station the wavelet dominating the trace around t=0 s is extracted and used for deconvolution. The construction of the wavelet used the full autocorrelation stack (i.e., positive and negative times). The time window of the wavelet was selected by visual inspection and it was selected to be 5s. This approach did not yield good results as it suppressed most of the reflectivity throughout the profile.

The second approach is based on the subtraction of the average delta pulse. To construct the wavelet, all the stations are stacked together. The selection of the time-window to extract the wavelet followed the same procedure as in the deconvolution approach. Then the wavelet is subtracted from each station stack. This approach seems to produce similar results as the deconvolution, except it preserves more reflectivity earlier than 5 s. Still, most of the coherent reflectivity was suppressed.

The selected technique to eliminate the delta pulse was muting. We selected the time window to be muted as in the other two procedures, but to keep it as possible. A window of 3 s was selected, even though the wavelet is probably slightly longer at the southern stations compared to the northern ones. This procedure preserved the reflectivity of the profile and was selected for that reason.

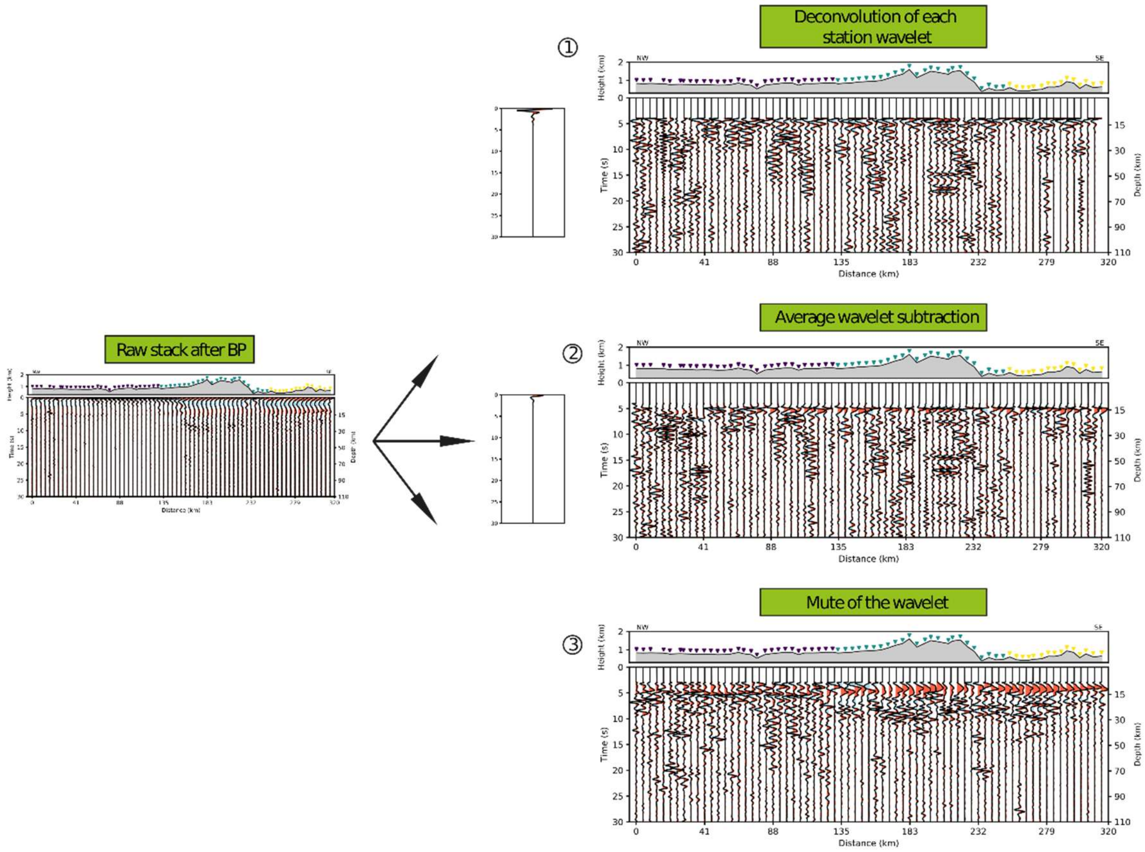

Figure S3. Approaches to eliminate the influence of the delta pulse at t=0. 1) deconvolution for each station of the wavelet, 2) subtraction of the average wavelet of all the station, 3) muting of the wavelet.

Table S1. Global earthquakes used in this study.

Date	Latitude (º)	Longitude (º)	Depth (km)	Magnitude	Deployment
24/05/2017	-10.0191	161.9535	52	5.5	Central
25/05/2017	-22.3132	-176.3299	127	5.6	Central
29/05/2017	-1.2923	120.4313	12	6.6	Central
30/05/2017	-12.113	167.266	257.42	5.2	Central
02/06/2017	-4.7348	145.1363	192.85	5.9	Central
03/06/2017	-62.5792	155.834	10	5.9	Central
09/06/2017	-16.855	-177.6	10	5.6	Central
09/06/2017	5.486	125.139	13.99	5.2	Central
09/06/2017	-10.26	161.185	53.2	5.2	Central
10/06/2017	-54.3039	-146.639	10	5.6	Central
10/06/2017	-11.503	166.433	48.46	5.1	Central
12/06/2017	3.69	126.776	56.82	5.4	Central
14/06/2017	-18.3246	168.728	13.6	5.8	Central
15/06/2017	-30.5156	-178.0563	34	6	Central
15/06/2017	-55.414	-124.789	10	5.8	Central
17/06/2017	-24.0927	179.6041	511	6.1	Central
17/06/2017	51.76	-173.371	29.46	5.3	Central
25/02/2018	-6.0699	142.7536	25.21	7.5	South
25/02/2018	-5.8339	142.263	10	5.7	South
26/02/2018	-5.4592	151.8089	20.16	5.6	South
26/02/2018	-6.3991	143.2581	9	5.9	South
26/02/2018	-6.4973	143.5497	22	5.8	South
26/02/2018	-2.7774	126.6859	9	6.1	South
26/02/2018	-6.5052	143.255	19	6.3	South
27/02/2018	-18.8679	169.2903	203	5.5	South
27/02/2018	-6.4033	143.0332	12	5.7	South
27/02/2018	-60.2494	150.7793	10	6.1	South
28/02/2018	-6.1696	142.4681	16	6.1	South
02/03/2018	-6.1353	130.2782	135	5.9	South
04/03/2018	-6.0741	142.7211	6	5.7	South
04/03/2018	-6.331	142.5994	10	6	South
06/03/2018	-6.2314	142.4131	10	5.5	South
06/03/2018	-6.3043	142.6116	20.49	6.7	South
07/03/2018	-5.4456	151.3913	50	5.6	South
08/03/2018	-3.3428	130.9337	10	5.6	South
08/03/2018	-4.3762	153.1996	22.86	6.8	South
09/03/2018	-4.2814	153.3875	30	5.8	South
09/03/2018	-21.0006	-178.606	540.34	5.7	South
12/03/2018	-46.3559	95.9296	10	5.6	South
22/03/2018	-30.1742	-177.7218	22.22	5.5	South
24/03/2018	-5.4959	151.4971	33	6.3	South
24/03/2018	-45.7783	96.0692	10	6	South

25/03/2018	-7.3049	128.4848	144	5.7	South
25/03/2018	-6.6343	129.8172	169	6.4	South
26/03/2018	-5.5024	151.4025	40	6.7	South
29/03/2018	-9.4211	159.5792	32	5.8	South
29/03/2018	-5.5321	151.4999	35	6.9	South
29/03/2018	-5.899	151.8542	10	5.7	South
02/04/2018	-24.719	-176.8865	92	6.1	South
05/04/2018	-18.2946	-177.9138	511	5.8	South
06/04/2018	-1.4171	138.2026	10	5.6	South
07/04/2018	-6.3608	142.6662	10	5.5	South
07/04/2018	-5.8382	142.5314	18.07	6.3	South
15/04/2018	1.4083	126.8759	34	6	South
17/04/2018	-3.5216	131.3032	10	5.5	South
06/07/2018	-49.6301	126.0404	10	5.5	North
07/07/2018	-30.5662	-178.0701	35	6	North
08/07/2018	-21.2766	168.4961	10	5.5	North
08/07/2018	-19.0182	169.4901	255	5.5	North
13/07/2018	-18.9279	169.0467	167	6.4	North
17/07/2018	-11.5936	166.432	37.96	6	North
20/07/2018	18.45	145.993	121	5.6	North
22/07/2018	-18.9577	168.8868	103.46	5.5	North
28/07/2018	-7.1039	122.7263	578.16	6	North
28/07/2018	-8.2395	116.508	14	6.4	North
05/08/2018	-8.2579	116.4403	34	6.9	North
10/08/2018	-62.6208	165.635	10	5.6	North
17/08/2018	-7.3718	119.8017	529	6.5	North
19/08/2018	-18.1132	-178.1523	600	8.2	North
19/08/2018	-18.4447	-177.6404	575.76	6.3	North
19/08/2018	-18.2293	-178.1002	537.63	5.6	North
19/08/2018	-18.2748	-178.3539	618.29	5.7	North
19/08/2018	-8.3366	116.5993	16	6.3	North
19/08/2018	-16.9783	-178.0332	415.6	6.8	North
19/08/2018	-8.319	116.6271	21	6.9	North
19/08/2018	-8.3511	116.5565	10	5.8	North
20/08/2018	-18.1559	-178.1888	526.17	5.5	North
21/08/2018	-16.0295	168.145	9	6.5	North
22/08/2018	-6.9675	155.7284	34	5.8	North
28/08/2018	-10.8859	124.1187	14	6.2	North
28/08/2018	-18.0299	-177.9387	600.62	5.7	North